Human Molecular Genetics, 2014, Vol. 23, No. 6 **1644–1655**
doi:10.1093/hmg/ddt556
Advance Access published on November 7, 2013

SIRT2 regulates ciliogenesis and contributes to abnormal centrosome amplification caused by loss of polycystin-1

Xia Zhou[1,2], Lucy X. Fan[1,2], Keguo Li[4], Ramani Ramchandran[4], James P. Calvet[2,3] and Xiaogang Li[1,2,3,*]

[1]Department of Internal Medicine [2]Kidney Institute and [3]Department of Biochemistry and Molecular Biology, University of Kansas Medical Center, Kansas City, KS 66160, USA [4]Department of Pediatrics, Medical College of Wisconsin, Milwaukee, WI 53226, USA

Received September 12, 2013; Revised October 28, 2013; Accepted October 30, 2013

The mechanisms underlying many of the human disease phenotypes associated with ciliary dysfunction and abnormal centrosome amplification have yet to be fully elucidated. Here, we present for the first time that SIRT2, a nicotinamide adenine dinucleotide (NAD)-dependent deacetylase, regulates ciliogenesis and centrosome amplification. Overexpression of SIRT2 in renal epithelial cells appeared to disrupt cilia formation, causing decreased numbers of cells with cilia and decreased cilia length, while inhibition of SIRT2 activity by nicotinamide treatment or knockdown of SIRT2 with siRNA was shown to block cilia disassembly during the cell cycle. Overexpression of SIRT2 in zebrafish decreased cilia numbers in Kupffer's vesicle, while morpholino knock down of SIRT2 increased cilia length. Aberrant centrosome amplification and polyploidy were seen with overexpression of SIRT2 in mouse inner medullary collecting duct 3 cells, similar to that observed following *Pkd1* knockdown. SIRT2 was up-regulated in both *Pkd1* mutant and knockdown cells. Depletion of SIRT2 prevented the abnormal centrosome amplification and polyploidy associated with loss of polycystin-1 (PC1) alone. Thus, we conclude that the aberrant centrosome amplification and polyploidy in *Pkd1* mutant or depleted cells was mediated through overexpression of SIRT2. Our results suggest a novel function of SIRT2 in cilia dynamics and centrosome function, and in ciliopathy-associated disease progression.

INTRODUCTION

Defects in cilia structure and their signaling components have been associated with a variety of human diseases or disorders, collectively known as ciliopathies. These include renal cystic diseases, retinal dystrophy, Bardet-Biedl syndrome, neurosensory impairment, diabetes, infertility and hypertension (1–4). Defects in centrosome number or centrosome function are associated with cancer, and developmental disorders correlated with reduced brain growth (5), as well as polycystic kidney disease (6).

Cilia and centrosomes interact with and share a common structure known as the centriole, a small organelle ($\sim$ 200 nm in diameter and $\sim$ 400 nm in length) consisting of a cylindrical array of nine triplet microtubules (7). Centrioles organize the formation of centrosomes and cilia, which are actively involved in cell division, polarity and motility. The centriole recruits pericentriolar material to form the centrosome, and one of the two centrioles in the centrosome differentiates to function as the basal body, a structure that organizes microtubule bundles to form cilia. Cilia can be either motile with a ring of nine doublet microtubules surrounding a central pair (9 + 2), or immotile, missing the central microtubule pair (9 + 0), such as primary cilia that exist on most cells. The assembly and disassembly of centrosomes and cilia are associated with the phases of the cell cycle.

The centrosome is duplicated only once to give rise to two centrosomes during a normal cell division cycle, so that centrosome number remains constant in the daughter cells. Interphase cells contain a single centrosome that is typically located near the nucleus. It contains a pair of centrioles that are oriented in a

*To whom correspondence should be addressed at: Department of Internal Medicine, and the Kidney Institute, University of Kansas Medical Center, Mail Stop 3018, 3901 Rainbow Blvd., Kansas City, KS 66160, USA. Tel: +1 9135882731; Fax: +1 9135889251; Email: xli3@kumc.edu

characteristic orthogonal arrangement and that function to anchor the recruitment of pericentriolar material, including the microtubule nucleating protein γ-tubulin (8). As cells pass through the G1 phase and enter the S phase of the cell cycle, the centrioles duplicate and lengthen. Centrosome duplication is completed during late G2/M and each new centrosome (i.e. mitotic spindle pole) contains one old (mother centriole) and one new (daughter) centriole. The presence of only two centrosomes in the cell as it enters the mitotic phase (prophase, metaphase, anaphase and telophase) ensures the equal segregation of sister chromatids to each daughter cell.

The primary cilium is assembled during the interphase and is disassembled during the mitotic phase. The formation of the primary cilium begins when the distal end of the mother centriole (now the basal body) attaches to and becomes enclosed by a membrane vesicle. The microtubule core (axoneme) of the cilium then assembles directly onto the microtubules of the centriole. As the axoneme lengthens, the primary ciliary vesicle enlarges and becomes a sheath. Eventually, the sheath fuses with the cytoplasmic membrane and the primary cilium protrudes from the cell surface (9). After the centrioles duplicate and lengthen during the S phase, ciliary shortening occurs during G2/M and eventually the primary cilium resorbs from the plasma membrane (10,11).

The stability and function of microtubules, components of both the centrosome and ciliary axoneme, are regulated by the status of tubulin acetylation and deacetylation (12). The acetyltransferase alphaTAT1, with a highly specific α-tubulin K40 acetyltranferase activity, is required for the acetylation of axonemal microtubules and for the normal assembly dynamics of primary cilia (13). Histone deacetylase 6 (HDAC6), which has a specific α-tubulin deacetylase activity, is required for destabilization of the microtubule-based axoneme and for cilia disassembly (14). The human NAD^+-dependent protein deacetylase SIRT2 also mediates deacetylation of α-tubulin, and regulates mitotic exit by affecting mitotic structures including the centrosome, mitotic spindle and midbody to regulate chromosomal segregation during mitosis to ensure normal cell division (15). Cell cultures overexpressing wild-type SIRT2 exhibit an increase in multinucleated cells. SIRT2 resides predominantly in the cytoplasm where it functions as a tubulin deacetylase. However, during the cell cycle, SIRT2 becomes enriched in the nucleus and is associated with mitotic structures, beginning with the centrosome during the prophase, the mitotic spindle during the metaphase and the midbody during cytokinesis (15). SIRT2 is proposed to partner with HDAC6 in deacetylating α-tubulin since α-tubulin binds to the SIRT2-HDAC6 complex *in vitro* (16,17). Based on these studies, we propose that SIRT2 may be a factor that regulates both centrosome amplification and ciliogenesis.

In this study, we found that overexpression of SIRT2 decreased the percentage of renal epithelial cells with cilia while inhibition of SIRT2 by nicotinamide (NIC) treatment or knockdown of SIRT2 with siRNA increased the percentage of cells with cilia by blocking the disassembly of cilia. Our *in vivo* data in zebrafish also support a role for SIRT2 regulating ciliogenesis in Kupffer's vesicle (KV). In addition, we found that overexpression of SIRT2 in mouse inner medullary collecting duct 3 (IMCD3) cells induced aberrant centrosome amplification and polyploidy, which was similar to that seen with loss of polycystin-1 (PC1) in these cells. We found that SIRT2 was up-regulated in *Pkd1* knockdown mouse IMCD3 cells and *Pkd1* knockout mouse kidney cells. Double knockdown of *Pkd1* and SIRT2 with shRNA in mouse IMCD3 cells significantly decreased the number of cells with centrosome defects compared with those transduced with *Pkd1* shRNA alone. These results suggest that SIRT2 is one of the factors responsible for aberrant centrosome amplification and polyploidy in polycystic kidney disease. Our results suggest a novel mechanism for SIRT2 in regulating cilia formation and disassembly, and in centrosome amplification and polyploidy.

RESULTS

Knockdown SIRT2 with siRNA or inhibition of SIRT2 with NIC blocks cilia disassembly

Although there is clear evidence demonstrating that cilia are assembled and disassembled dynamically as cells progress through the cell cycle, the mechanisms by which this is controlled remain poorly understood. HDAC6 has been suggested to play a key regulatory role in the dynamic stability of microtubules through deacetylation of α-tubulin (12). HDAC6-mediated deacetylation of α-tubulin has also been found to regulate cilia disassembly during the normal cell cycle (14). We hypothesized that SIRT2, the only α-tubulin deacetylase of the sirtuin family proteins and a binding partner of HDAC6, may also regulate cilia disassembly. We found that SIRT2 co-localized with α-tubulin and formed a complex with α-tubulin in mouse IMCD3 cells as examined by immunostaining (Fig. 1A) or by immunoprecipitation (Fig. 1B), respectively. Knockdown of SIRT2 with siRNA increased the acetylation level of α-tubulin (Fig. 1C). In addition, treatment with NIC, a general sirtuin activity inhibitor, also increased the acetylation level of α-tubulin (Fig. 1D). These results suggested that SIRT2 deacetylated α-tubulin in mouse IMCD3 cells, and that this process could be inhibited by NIC.

It has been reported that serum starvation promotes cilia formation while re-feeding the starved cells with serum induces the process of ciliary disassembly (14). First, to determine the role of SIRT2 in this process, we induced cilia formation in mouse IMCD3 cells by serum starvation for 48 h, together with or without NIC and examined the cilia by anti-acetyl-α-tubulin antibody staining. We found that serum starvation alone for 48 h induced cilia formation in 79% of these mouse IMCD3 cells. Serum starvation together with NIC co-treatment further increased cilia formation in these cells to ∼94% (Fig. 2A). Serum starvation together with NIC co-treatment also increased cilia length in mouse IMCD3 cells (Fig. 2A). Although acetylated tubulin is a widely used marker for cilia, its use in this study may be challenged because SIRT2 is a tubulin deacetylase. Thus, we repeated the above experiments with another cilia marker, ARL13B (18), to score the percentage and length of cilia. We obtained similar results with these two cilia markers (Fig. 2A and B) and found that cilia stained with ARL13B exactly overlapped with cilia stained with acetyl-α-tubulin in mouse IMCD3 cells treated with or without NIC (Supplementary Material, Fig. S1A). These results suggested that either acetyl-α-tubulin or ARL13B could be used as a cilia marker despite the fact that inhibition of SIRT2 with NIC increased

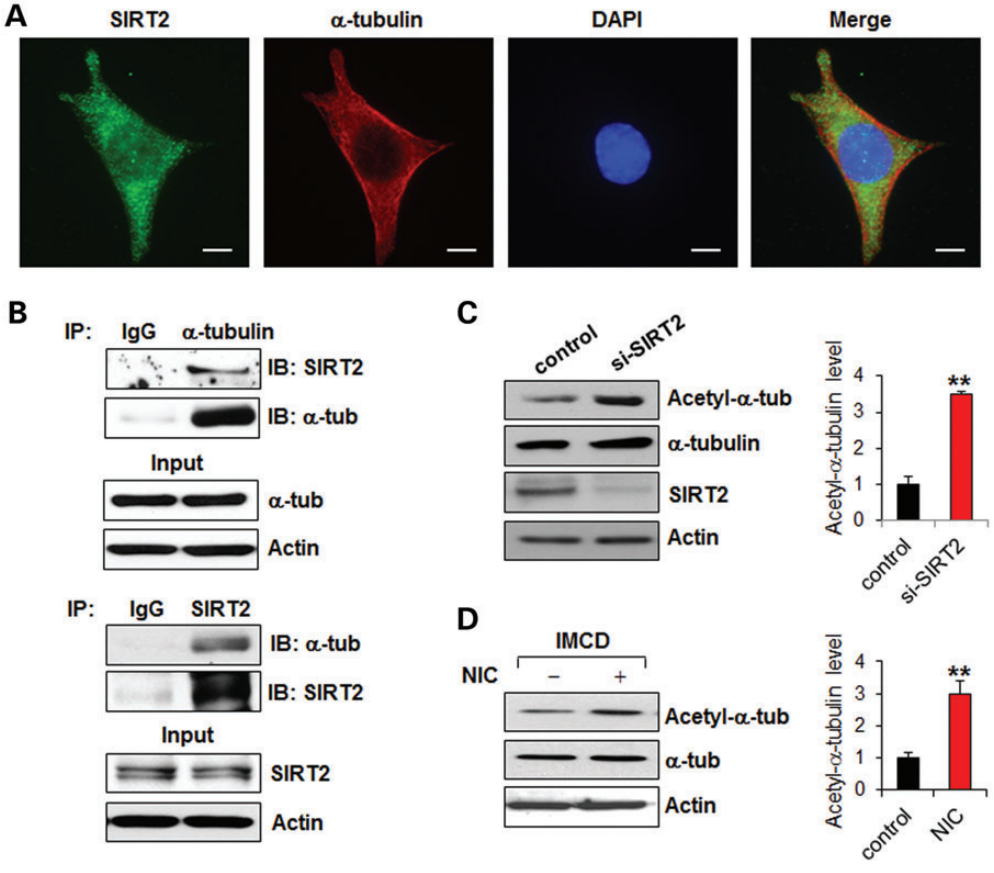

Figure 1. SIRT2 interacts with and deacetylates α-tubulin in mouse IMCD3 cells. (**A**) SIRT2 colocalized with α-tubulin in mouse IMCD3 cells as shown by co-staining with anti-SIRT2 and anti-α-tubulin antibodies. Scale bar, 10 μm. (**B**) SIRT2 interacts with α-tubulin in mouse IMCD3 cells as shown by immunoprecipitation with anti-α-tubulin antibody and anti-SIRT2 antibody, respectively. (**C**) Knockdown of SIRT2 with siRNA increased the level of acetyl-α-tubulin in mouse IMCD3 cells as shown by western blotting analysis. (**D**) NIC treatment increased the level of acetyl-α-tubulin in mouse IMCD3 cells as shown by western blotting analysis. The expression of acetyl-α-tubulin was quantified from three independent immunoblots and is presented as the relative acetyl-α-tubulin level standardized to actin. $^{**}P < 0.01$.

the levels of acetyl-α-tubulin (Fig. 1D). We further found that knockdown of SIRT2 with siRNA increased the percentage of cells with cilia and cilia length as scored with the above two cilia markers (Fig. 2C–E). In addition, we found that SIRT2 localized to the basal body of cilia in mouse IMCD3 cells without NIC treatment, following serum starvation for 48 h (Fig. 2F and G) and that treatment with NIC did not affect the basal body localization of SIRT2 in mouse IMCD3 cells, following serum starvation for 48 h (Supplementary Material, Fig. S2). However, knockdown of SIRT2 with siRNA completely abolished the appearance of SIRT2 in the cytosol and at the basal body, confirming the specificity of the anti-SIRT2 antibody for immunostaining (Fig. 2G). These results suggested that SIRT2-mediated deacetylation of α-tubulin might regulate the ciliary assembly/disassembly process.

Next, to determine the role of SIRT2 in cilia disassembly, we induced cilia disassembly in serum-starved mouse IMCD3 cells by re-feeding with serum. Two hours before being re-fed with serum, cells were treated with or without NIC. We found that after 48 h of serum starvation followed by re-feeding with serum in the absence of NIC, the cilia gradually resorbed over a period of 12 h. (Fig. 3A, black bars in *top panel*). However, this ciliary disassembly was completely blocked in these cells after re-feeding with serum and NIC as analyzed by anti-acetyl-α-tubulin antibody staining (Fig. 3A, gray bars in *bottom panel*) or by anti-ARL13B antibody staining (Fig. 3B, gray bars in *right panel*). We further found that depletion of SIRT2 by shRNA blocked cilia resorption in cells, following re-feeding with serum (Fig. 3C).

To exclude the possibility that NIC treatment or knockdown of SIRT2 blocked cilia disassembly by inhibiting cell cycle re-entry, we performed BrdU incorporation assays. We found that the percentage of BrdU-positive cells, which represents the proliferating cells, was subtly increased at 6 h after serum re-feeding and strikingly increased at 12 h after serum re-feeding in cells treated with NIC or transfected with SIRT2 shRNA, similar to control untreated or control vector transfected cells (Supplementary Material, Fig. S3A and B). The BrdU incorporation assay results indicated that neither NIC treatment nor knockdown SIRT2 with shRNA influenced S phase entry during this 12-h serum re-feeding period. It has been reported that treatment with a general HDAC inhibitor, Trichostatin A (TSA), or a specific HDAC6 inhibitor, tubacin, blocks serum-induced ciliary disassembly (14). We also found that TSA and tubacin-blocked ciliary disassembly in mouse IMCD3 cells under conditions of serum re-feeding (data not shown). These

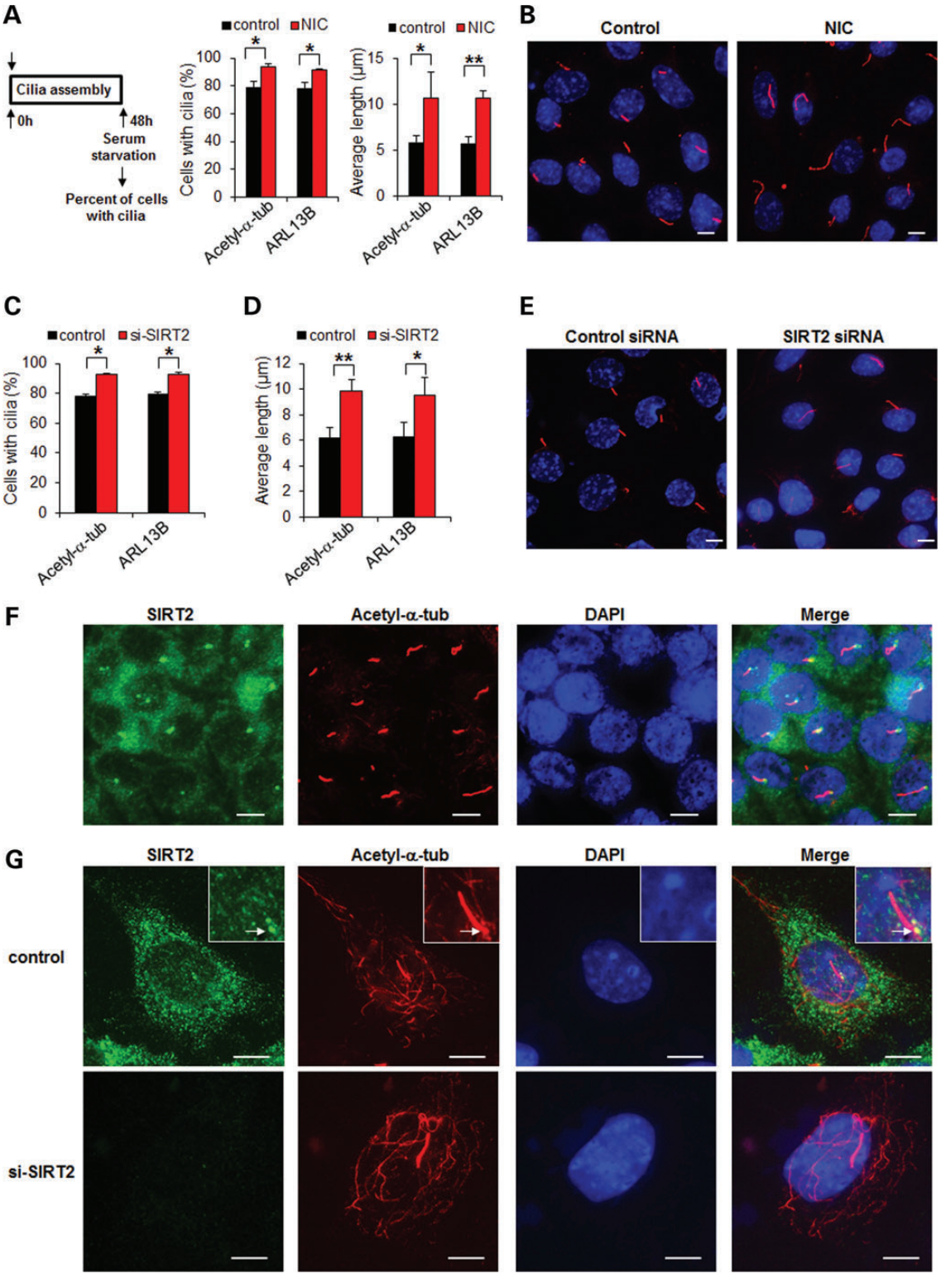

Figure 2. Inhibition of SIRT2 with NIC or knockdown of SIRT2 with siRNA increases cells with cilia and cilia length. (**A**) Mouse IMCD3 cells were starved for 48 h with or without 10 mM NIC and then stained with two cilia markers, anti-acetyl-α-tubulin antibody or anti-ARL13B antibody, respectively. The percentage of cells with cilia was counted, and the lengths of the cilia were measured. The assay was performed three times, with an average of 200 cells counted. $^{*}P < 0.05$. $^{**}P < 0.01$. (**B**) The cilia on serum-starved mouse IMCD3 cells with or without NIC treatment were stained by anti-ARL13B antibody (*red*) and nuclei were stained with DAPI (*blue*). (**C** and **D**) Mouse IMCD3 cells transfected with SIRT2 siRNA and starved for 48 h were stained with anti-acetyl-α-tubulin antibody and anti-ARL13B antibody, to score the percentage of cells with cilia (**C**) and the lengths of the cilia (**D**). $^{*}P < 0.05$. $^{**}P < 0.01$. (**E**) The cilia in the serum-starved mouse IMCD3 cells transfected with SIRT2 siRNA were stained with anti-ARL13B antibody. (**F**) SIRT2 localized at the basal body of cilia. Mouse IMCD3 cells were starved for 48 h and were immunostained with anti-SIRT2 antibody (*green*), anti-acetyl-α-tubulin antibody (*red*) and counterstained with DAPI (*blue*). Scale bar, 10 μm. (**G**) The mouse IMCD3 cells transfected with SIRT2 siRNA were stained with anti-SIRT2 antibody (*green*) and anti-acetyl-α-tubulin antibody (*red*) and counterstained with DAPI (*blue*). Arrows point basal body. Scale bar, 10 μm.

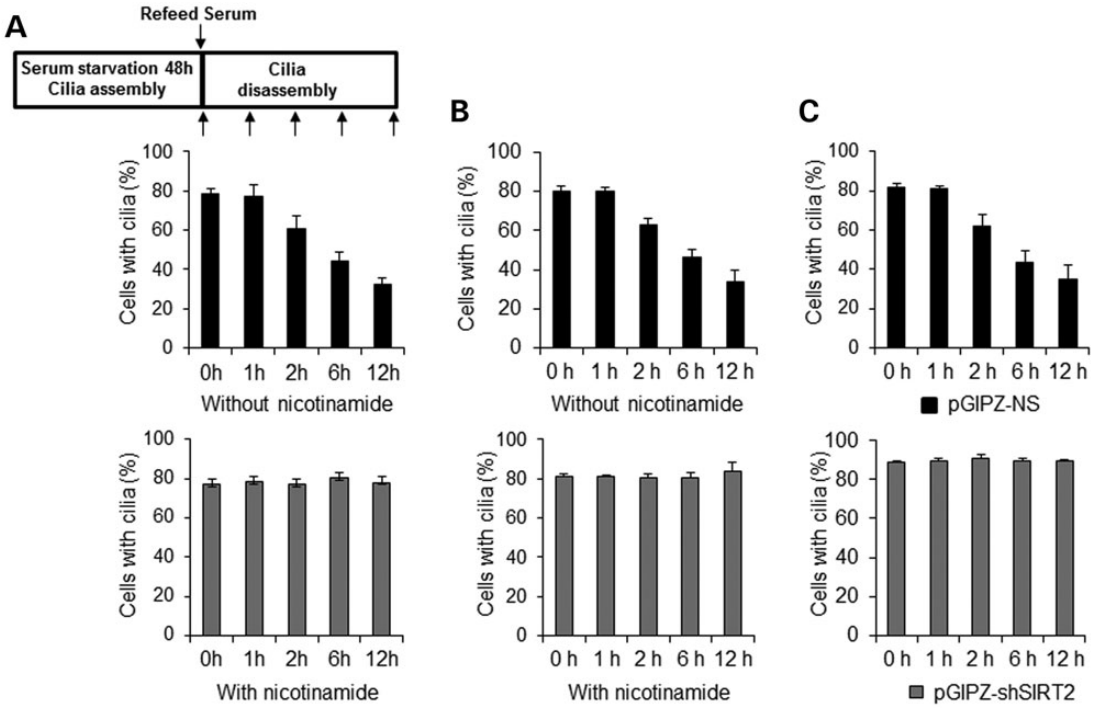

Figure 3. Inhibition of SIRT2 with NIC or knockdown of SIRT2 with shRNA inhibits cilia disassembly. (**A** and **B**) Treatment of mouse IMCD3 cells with NIC prevents ciliary resorption. Cells were plated at 30% confluence in medium without serum for 48 h, and were stained after serum addition at 0–12 h. Cells were incubated with 10 mM NIC for 2 h prior to induction of ciliary disassembly. The percentage of cells with cilia was counted at the indicated time points stained with either anti-acetyl-α-tubulin antibody (**A**) or anti-ARL13B antibody (**B**). The assay was performed three times, with an average of 200 cells counted/time point. (**C**) Depletion of SIRT2 with shRNA prevents ciliary resorption in mouse IMCD3 cells. Mouse IMCD3 cells transduced with SIRT2 shRNA or control vector were plated at 30% confluence in medium without serum for 48 h, and were stained after serum addition at 0–12 h. The percentage of cells with cilia was counted at the indicated time points stained with anti-ARL13B antibody.

results suggested that SIRT2 regulates cilia disassembly during the cell cycle and thus functionally overlaps with HDAC6.

Overexpression of SIRT2 decreases cilia number and length in mouse IMCD3 cells

To further investigate whether SIRT2 regulation of α-tubulin acetylation affects cilia formation, we transiently transfected (green fluorescent protein) GFP-SIRT2 into mouse IMCD3 cells for 24 h and then counted the percentage of cells with cilia after another 48 h of serum starvation. Compared with GFP vector-transfected cells, overexpressing SIRT2 significantly reduced the percentage of cells with cilia (Fig. 4A). In contrast, transfection of the SIRT2 deacetylase-inactive mutant (H187Y) did not decrease the percentage of cells with cilia (Fig. 4A). GFP-SIRT2 stably transfected mouse IMCD3 cells also showed a decreased percentage of cells with cilia (Fig. 4B and 4D). Furthermore, we found that the lengths of cilia on the GFP-SIRT2 stably transfected cells were strikingly reduced (Fig. 4C and D), together with decreased levels of acetylated α-tubulin (Fig. 4E). These results suggest that overexpression of SIRT2 disrupts cilia formation and that this process may be regulated through SIRT2-mediated deacetylation of α-tubulin.

SIRT2 regulates cilia number and length in KV of zebrafish embryos

To examine the functional role of SIRT2 in ciliogenesis *in vivo*, we determined the effects of overexpression or knockdown of SIRT2 on ciliogenesis in the KV of zebrafish. The KV is a fluid-filled organ with ciliated epithelium, which regulates left-right asymmetry by establishing a directional fluid flow during development (19). The KV is formed from dorsal forerunner cells at the 4- to 5-somite stage (SS) and is present during most of the segmentation period (19). First, we injected zebrafish embryos with mouse wild-type or deacetylase-inactive mutant SIRT2 mRNA, and performed immunostaining with anti-acetyl-α-tubulin antibody at the 10-SS. We found that the cilia in KVs were significantly reduced in wild-type SIRT2 overexpressing embryos ($n = 31$) compared with that in control embryos ($n = 22$) (Fig. 5A and B). In contrast, the SIRT2 deacetylase-inactive mutant H187Y was unable to decrease cilia number ($n = 11$) (Fig. 5A and B). Second, we found that knockdown of zebrafish SIRT2 by injecting zebrafish embryos with a SIRT2 morpholino, which was confirmed by reverse transcription PCR (Fig. 5C), resulted in longer cilia at the 10-SS compared with that in age-matched control injected embryos (Fig. 5D and E). The elongated cilia phenotype could not be rescued by co-injecting mouse wild-type SIRT2 (data not shown). Morpholino knockdown of SIRT2 through targeting two different regions of SIRT2 mRNA increased cilia length in KVs (Fig. 5E and Supplementary Material, Fig. S4C), which suggested that the observed phenotype was not due to off-target effects, and had no significant effect on cilia number in KV ($n = 10$) (Fig. 5F and Supplementary Material, Fig. S4D), These results suggest that there is a critical role for SIRT2 in the formation of cilia *in vivo*.

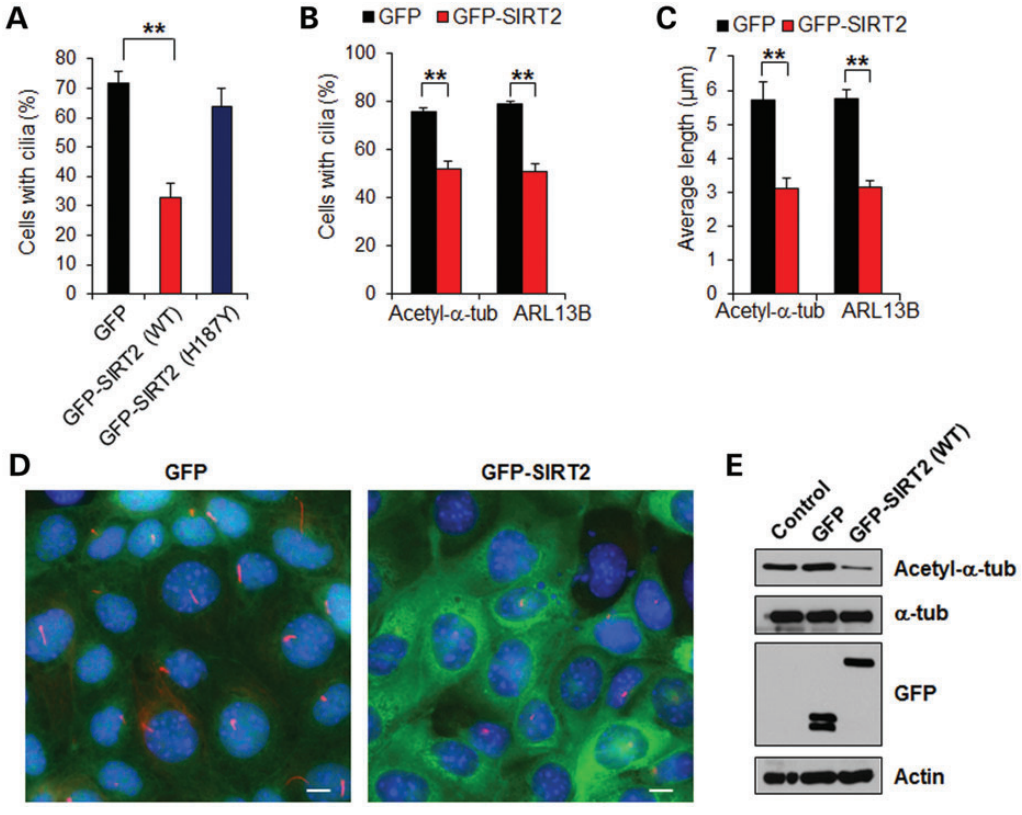

Figure 4. Overexpression of SIRT2 decreases cilia number and length. (**A**) Mouse IMCD3 cells were transiently transfected with green fluorescent protein (GFP), GFP-SIRT2 (WT) and GFP-SIRT2 (H187Y), respectively; 24 h after transfection, the cells were cultured in medium without serum for 48 h. The cilia in GFP-positive cells were visualized with acetyl-α-tubulin antibody. An average of 200 cells was counted in each of three experiments. $^{**}P < 0.01$. (**B** and **C**) The percentage of cells with cilia was counted (B), and the lengths of the cilia on ciliated cells were measured and presented as the average cilia length (C) in mouse IMCD3 cells stably transfected with GFP or GFP-SIRT2 stained with anti-acetyl-α-tubulin antibody and anti-ARL13B antibody, respectively. $^{**}P < 0.01$. (**D**) Mouse IMCD3 cells stably transfected with GFP or GFP-SIRT2 (WT) were cultured in medium without serum for 48 h, then cells were stained with anti-acetyl-α-tubulin antibody (*red*) and counterstained by DAPI (*blue*). (**E**) The level of acetyl-α-tubulin was increased in mouse IMCD3 cells with stable expression of GFP-SIRT2. Western blots were performed on mouse IMCD3 cell lysates stably expressing GFP or GFP-SIRT2 (WT), and were probed with acetyl-α-tubulin, α-tubulin and GFP antibodies.

Chromosome segregation defects and polyploidy caused by loss of PC-1 are mediated through SIRT2 up-regulation

It has been reported that knockdown of *Pkd1* in mouse IMCD3 cells and in endothelial cells results in abnormal centrosome amplification and multipolar spindle formation, which leads to genomic instability characterized by polyploidy and mitotic catastrophe (6,20). However, the molecular mechanisms leading to this abnormal centrosome amplification downstream of *Pkd1* loss is unknown. We confirmed that the loss of PC1, mediated by lentiviral shRNA knockdown in mouse IMCD3 cells (pGIPZ-shPkd1), leads to abnormal centrosome amplification (Supplementary Material, Fig. S5A) and multinucleation (Supplementary Material, Fig. S5B). Abnormal centrosome amplification was also detected in kidney tissues from $Pkd1^{flox/flox}$:*Ksp-Cre* mice (Supplementary Material, Fig. S5C) and ADPKD patients (Supplementary Material, Fig. S5D), respectively. Knockdown of *Pkd1* in mouse IMCD3 cells with lentiviral vector-mediated shRNAs (pGIPZ-shPkd1) increased the expression of SIRT2 compared with control cells transduced with the pGIPZ-NS vector (Fig. 6A). We further found that SIRT2 was up-regulated in *Pkd1* mutant mouse embryonic kidney (MEK) cells (null) compared with *Pkd1* wild-type MEK cells (Fig. 6B). In addition, we found that SIRT2 was enriched in the centrosome, as determined by its colocalization with the centrosome marker, γ-tubulin, in mouse IMCD3 cells at the interphase (Fig. 6C, *top panel*) and during mitosis (Fig. 6C, *bottom panel*), as well as in *Pkd1* mutant MEK cells (Supplementary Material, Fig. S6). These results suggest that mutation or knockdown of *Pkd1* can induce abnormal centrosome amplification and multipolar spindle formation, and that this process may be regulated by increased SIRT2.

To evaluate whether SIRT2 affects centrosome amplification and polyploidy, we overexpressed SIRT2 in mouse IMCD3 cells and stained the cells using anti-pericentrin antibody to mark the centrosome. We found that in GFP-SIRT2 transiently transfected cells, GFP-SIRT2 co-localized with centrosome pericentrin staining (Fig. 7A). Overexpression of wild-type GFP-SIRT2 (WT) in mouse IMCD3 cells resulted in the formation of multiple centrosomes (Fig. 7A) and multinucleation (Fig. 7B and C, $P < 0.01$). In contrast, the inactive SIRT2 (H187Y) mutant did not induce multinucleation in transient transfected mouse IMCD3 cells (Fig. 7B and C). Inhibition of SIRT2 activity by NIC could decrease multinucleation in SIRT2 overexpressing mouse IMCD3 cells in a dose-dependent manner (Fig. 7D, $P < 0.01$).

To examine whether abnormal centrosome amplification induced by loss of PC1 is mediated through overexpression of

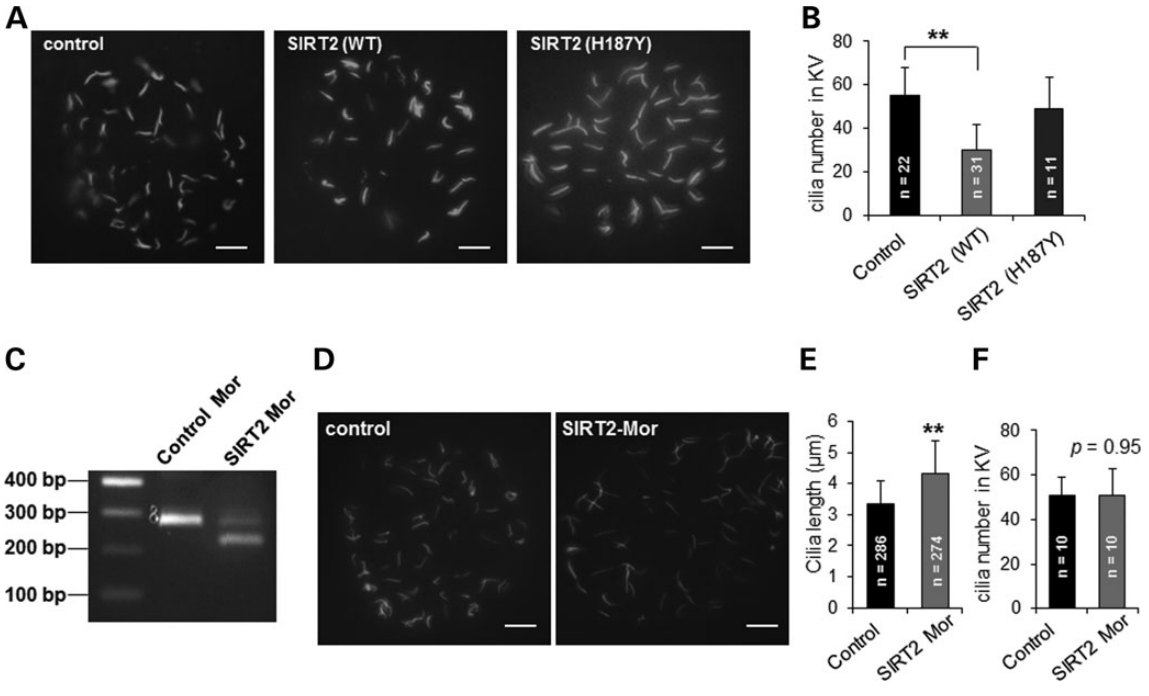

Figure 5. SIRT2 regulates cilia number and length in KV of zebrafish embryos. (**A**) Whole-mount immunofluorescence microscopy of cilia at the KV of embryos injected with SIRT2 wild-type mRNA or SIRT2 (H187Y) mRNA at the one-cell stage, then examined at the 10-SS using antibody against acetyl-α-tubulin (*green*). Scale bar, 5 μm. (**B**) Cilia numbers in KV in indicated embryos at the 10 SS. Error bar shows SD. $^{**}P < 0.01$. (**C**) The knockdown efficiency of SIRT2 morpholino (Mor) targeting exon 3 and intron 3 splice site was analyzed by reverse transcription PCR. (**D**) Whole-mount immunofluorescence microscopy of cilia at the KV in embryos at the 10 SS, injected with control or SIRT2 morpholino. Scale bar, 5 μm. (**E**) Cilia lengths in KV were measured at the 10 SS embryos injected with control or SIRT2 morpholino respectively. *n* represents total cilia numbers that were measured for cilia length from 6 embryos per group. $^{**}p < 0.01$. (**F**) Cilia numbers in KV ($n = 10$) at the 10 SS embryos injected with control or SIRT2 morpholino, respectively.

SIRT2, we knocked down both *Pkd1* and SIRT2 with shRNA in mouse IMCD3 cells. We found that depletion of both SIRT2 and *Pkd1* prevented abnormal centrosome amplification induced by loss of PC1 alone (Fig. 8A, $P < 0.01$). Depletion of SIRT2 alone did not induce abnormal centrosome amplification (Fig. 8A). Knockdown of *Pkd1* increased the levels of SIRT2 and decreased the levels of acetylated α-tubulin, while knockdown SIRT2 alone or double knockdown of *Pkd1* and SIRT2 decreased the levels of SIRT2 and increased the levels of acetylated α-tubulin (Fig. 8B). We further found that inhibition of SIRT2 with NIC decreased the percentage of cells with abnormal centrosome amplification caused by *Pkd1* shRNA knockdown (Fig. 8C, $P < 0.01$). Although the level of SIRT2 was up-regulated, the level of acetylated α-tubulin was also increased in *Pkd1* shRNA knockdown cells treated with NIC (Fig. 8D). On the basis of these data, we conclude that abnormal centrosome amplification and polyploidy induced by loss of PC1 is mediated through up-regulated SIRT2.

DISCUSSION

Centrosomes and cilia share a commonality in structure, composition and function. While a variety of factors associated with either ciliogenesis or centrosome amplification have been reported, no single factor regulating both processes was previously identified. In this study, we present evidence that SIRT2 regulates both ciliogenesis and centrosome amplification, and thus may be a factor in ciliopathies, including polycystic kidney disease and cancer. We demonstrate that overexpression of SIRT2 causes (i) decreased numbers of mouse IMCD3 cells with cilia; (ii) decreased cilia number in KV in zebrafish and (iii) aberrant centrosome amplification and polyploidy in mouse IMCD3 cells. We also show that inhibition of SIRT2 with NIC or siRNA blocks cilia disassembly, and that morpholino knockdown of SIRT2 increases cilia length in KV. In addition, we found that SIRT2 was up-regulated in *Pkd1* knockdown mouse IMCD3 cells and *Pkd1* knockout mouse kidney cells, and that the aberrant centrosome amplification and polyploidy induced by loss of PC1 is mediated through SIRT2 up-regulation.

Cilia have been known to be dynamically resorbed and resynthesized during the cell cycle (21). Primary cilia are disassembled as cells re-enter the cell cycle prior to mitosis and, in some cases, prior to the S phase. It has been suggested that cilia disassembly can be initiated by aurora A, a centrosomal kinase whose activity regulates entry into mitosis through the activation of cyclin-dependent kinase 1 (CDK1)-cyclin B, and mediates phosphorylation of HDAC6, which then acts on α-tubulin (14). Depletion of aurora A or its activator, human enhancer of filamentation 1 (HEF1) or administration of aurora A inhibitors or HDAC6 inhibitors prevent cilia disassembly (14). A model of cilia disassembly has been proposed in which aurora A activates ciliary HDAC6, which in turn deacetylates axonemal microtubules, leading to the rapid collapse of the primary cilium (14). However, this model is challenged by the finding that knocking out the *Hdac6* gene in mice produces

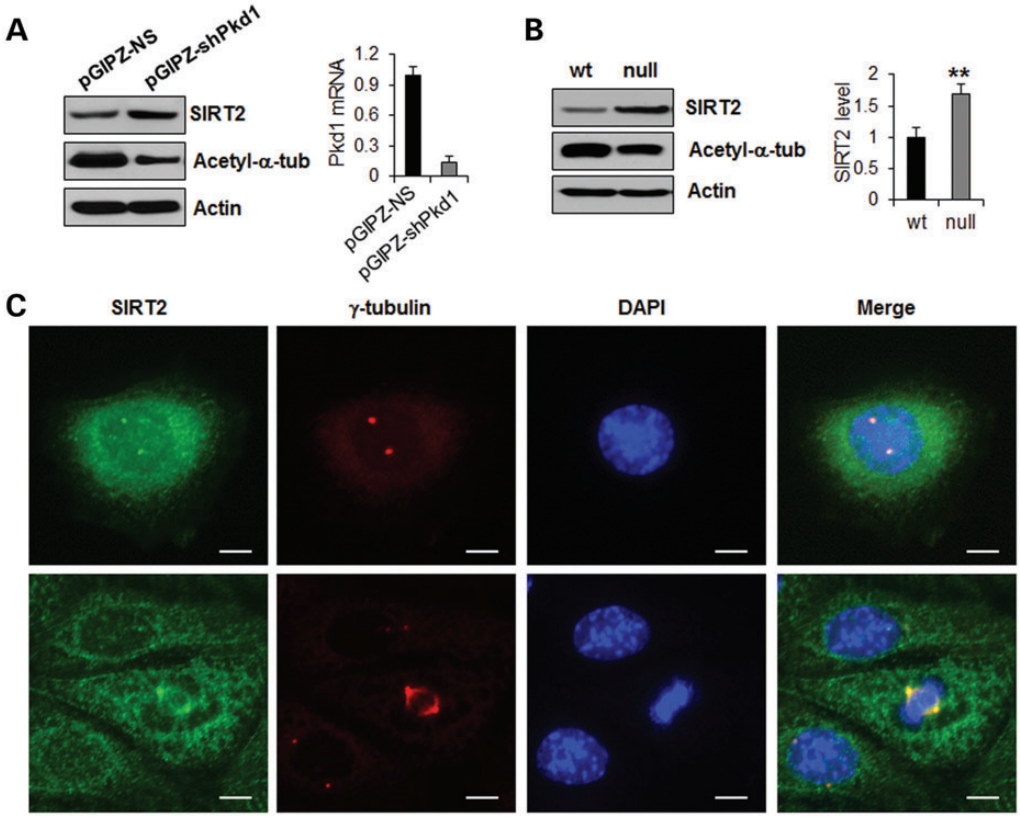

Figure 6. SIRT2 is up-regulated in *Pkd1* knockdown or *Pkd1* knockout renal epithelial cells. (**A**) SIRT2 was up-regulated and acetylated α-tubulin was decreased in Lentivector-mediated *Pkd1* knockdown mouse IMCD3 cells. Mouse IMCD3 cells were transduced with Lentivector-mediated *Pkd1* shRNAs, pGIPZ–shPkd1, and the control vector, pGIPZ-NS, respectively. The expression of SIRT2 in these cells was analyzed by western blot (*left panel*). The *Pkd1* knockdown efficiency was evaluated with qRT–PCR, which indicated that *Pkd1* expression was reduced by >85% in pGIPZ–shPkd1 transduced IMCD3 cells compared with that in control pGIPZ-NS transduced cells (*right panel*). (**B**) Western blot analysis of the expression of SIRT2 and acetylated α-tubulin from whole cell lysates of *Pkd1* wild-type (wt) and *Pkd1*$^{null/null}$ (null) MEK cells. SIRT2 was up-regulated and acetylated α-tubulin was decreased in *Pkd1* null MEK cells compared with *Pkd1* wild-type cells. The expression of SIRT2 was quantified from three independent immunoblots and was presented as the relative SIRT2 expression level standardized to actin in the right panel. $^{**}P < 0.01$. (**C**) SIRT2 localized at centrosome in both interphase (*upper panel*) and mitotic (*lower panel*) mouse IMCD3 cells. Mouse IMCD3 cells were immunostained with anti-SIRT2 (*green*) antibody and anti-γ-tubulin (*red*) antibody, a centrosome marker. Scale bar, 10 μm.

only subtle phenotypes affecting the immune response and bone density rather than gross abnormalities and embryonic lethality (22), which would be expected if a lack of this protein caused hyperstable microtubules or persistent cilia. Our finding that SIRT2 regulates cilia disassembly and the fact that SIRT2 is able to form a complex with HDAC6 suggest that SIRT2 regulates cilia size together with HDAC6 (Figs 2 and 3) (16). However, our results that inhibition of either SIRT2 or HDAC6 alone is sufficient to induce hyperacetylation of α-tubulin and that inhibition blocks cilia disassembly (Fig. 3) (16) suggest that the function of SIRT2 to regulate ciliogenesis is independent of HDAC6. These results may explain the result that knockout of HDAC6 does not cause hyperstable microtubules or persistent cilia since SIRT2 may compensate for the loss of HDAC6 in knockout cells and organs. The observation that SIRT2 is localized in centrosomes together with aurora A (14,15) and that SIRT2 immunoprecipitates with aurora A (23) further supports this idea. Whether the effect of SIRT2 on cilia disassembly is regulated by aurora A-mediated phosphorylation during the normal cell cycle and what role, if any, α-tubulin acetylation has in antagonizing this process needs to be further investigated.

Phosphorylation and dephosphorylation of SIRT2 is regulated by Cdk1 and the phosphatase CDC14B, respectively (24,25). Knockdown of CDC14B in zebrafish has been reported to inhibit ciliogenesis, as shown by the presence of shorter cilia in CDC14B-deficient embryos (26). Our results that overexpression of SIRT2 decreased cilia numbers in KV in zebrafish (Fig. 5) suggested that SIRT2 may be one of the downstream targets of CDC14B-mediated ciliogenesis. If so, knockdown of CDC14B might cause short cilia by increasing the levels of phosphorylated SIRT2, thus increasing its α-tubulin deacetylase activity.

Ciliogenesis and cell cycle progression are mutually exclusive processes (27). However, recent findings support a network connection between these events. It has been reported that the centrosomal protein nuclear distribution E homologue 1 (Nde1) negatively regulates ciliary length and cell cycle re-entry (28). Nde1 was detected at high levels in the mitotic phase but decreased to low levels in quiescent cells. Nde1 localized at the mother centriole, which organizes microtubule bundles to form the primary cilia. Depletion of Nde1 results in longer cilia and a delay in cell cycle re-entry, which suggests a correlation between ciliary length and cell cycle progression. Tctex-1 (or DYNLT), a light chain subunit of cytoplasmic

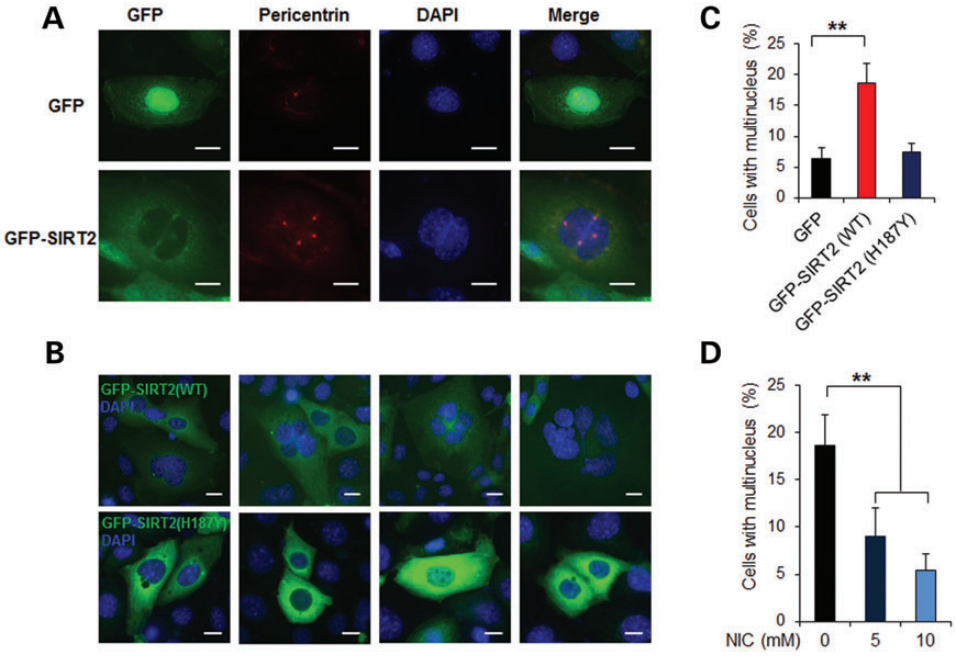

Figure 7. Overexpression SIRT2 leads to aberrant centrosome amplification and polyploidy. (**A**) Overexpression SIRT2 in mouse IMCD3 cells leads to aberrant centrosome amplification. Mouse IMCD3 cells transfected with (green fluorescent protein) GFP-SIRT2 (WT) or GFP were immunostained for pericentrin (*red*) to visualize the centrosomes and were counterstained with DAPI (*blue*). Scale bar, 10 μm. (**B** and **C**) Overexpression SIRT2 in mouse IMCD3 cells results in multinucleation. Mouse IMCD3 cells were transfected with GFP, GFP-SIRT2 (WT) or GFP-SIRT2 (H187Y), respectively; 48 h after transfection, cells were scored for the presence of multiple nuclei (**C**). An average of 200 cells was counted. Error bars show the SD. $^{**}P < 0.01$. Scale bar, 10 μm. (**D**) NIC inhibits SIRT2-induced polyploidy in mouse IMCD3 cells. Mouse IMCD3 cells were transfected with GFP-SIRT2 (WT) together with 5 or 10 mM NIC; 48 h after transfection, cells were scored for the presence of multiple nuclei. An average of 200 cells was counted. $^{**}P < 0.01$; one-way ANOVA.

dynein, which can perform dynein-dependent or dynein-independent (uncoupled from the dynein complex) functions (29), also has a key role in cilia-dependent S-phase entry (30). In addition, cilia assembly associated proteins, including IFT88 (intraflagellar transport protein 88) and IFT27 (intraflagellar transport protein 27), are also able to affect the cell cycle (31,32). These studies suggest that cilia may act as a brake to regulate the cell cycle (33).

SIRT2 was up-regulated in *Pkd1* mutant MEK cells when compared with wild-type cells (Fig. 5), suggesting that SIRT2 might affect ciliogenesis in *Pkd1* mutant kidney tissues. We found that cilia were present on cystic epithelial cells in *Pkd1* mutant kidneys (data not shown). Most common were short, bar-like cilia; however, abnormally long cilia were also observed. While there are observations to the contrary (34), abnormally long cilia have been seen in the cystic kidneys of a *Pkd1* mutant mouse (35). Thus, it is possible that up-regulation of SIRT2 induced by PC1 loss leads to a structural ciliogenesis defect in *Pkd1* mutant renal tissues.

Loss of PC1 in renal epithelial cells and in endothelial cells has been reported to induce centrosome amplification and multipolar spindle formation, leading to genomic instability (6,20). However, the mechanism underlying loss of PC1-mediated centrosome amplification and polyploidy is unknown. Our observations that knockdown of *Pkd1* in mouse IMCD3 cells causes up-regulation of SIRT2 (Fig. 6A), that overexpression of SIRT2 causes aberrant centrosome amplification and polyploidy (Fig. 7), and that depletion of SIRT2 prevents loss of PC1-induced aberrant centrosome amplification and polyploidy (Fig. 8), suggests that aberrant centrosome amplification and polyploidy caused by loss of PC1 is mediated through abnormal up-regulation of SIRT2. This conclusion is also supported by findings that cells exogenously expressing SIRT2 exhibit a marked prolongation of the mitotic phase of the cell cycle (24). Thus, a possible mechanism for the polyploidy induced in *Pkd1* knockdown cells is that up-regulated SIRT2 disrupts chromosome segregation through an alteration of the α-tubulin acetylation status (Fig. 8B), which results in insufficient separation of centriole pairs and aberrant centrosome amplification. However, interpretation of these data is complicated by another study in which knockdown SIRT2 in mouse embryonic fibroblast (MEF) cells induced centrosome amplification associated with increased expression of aurora A (23). A possible interpretation for these apparent gain- and loss-of-function actions of SIRT2 in centrosome amplification is that overexpression of SIRT2 in renal epithelial cells may activate specific pathway(s) or the ectopic activity of protein(s), such as α-tubulin, while knockdown SIRT2 in MEF cells may impair specific pathway(s), such as APC/C signaling (23), leading to increased levels of aurora A which is required for centrosome maturation and separation (36,37), with abnormal centrosome amplification consequences. Centrosome overduplication generally induces uneven chromosomal segregation and greater cellular DNA content, multipolar spindles, misalignment of chromosomes and incomplete cytokinesis. The association of cytokinesis defects with aberrant centrosome amplification and defects of

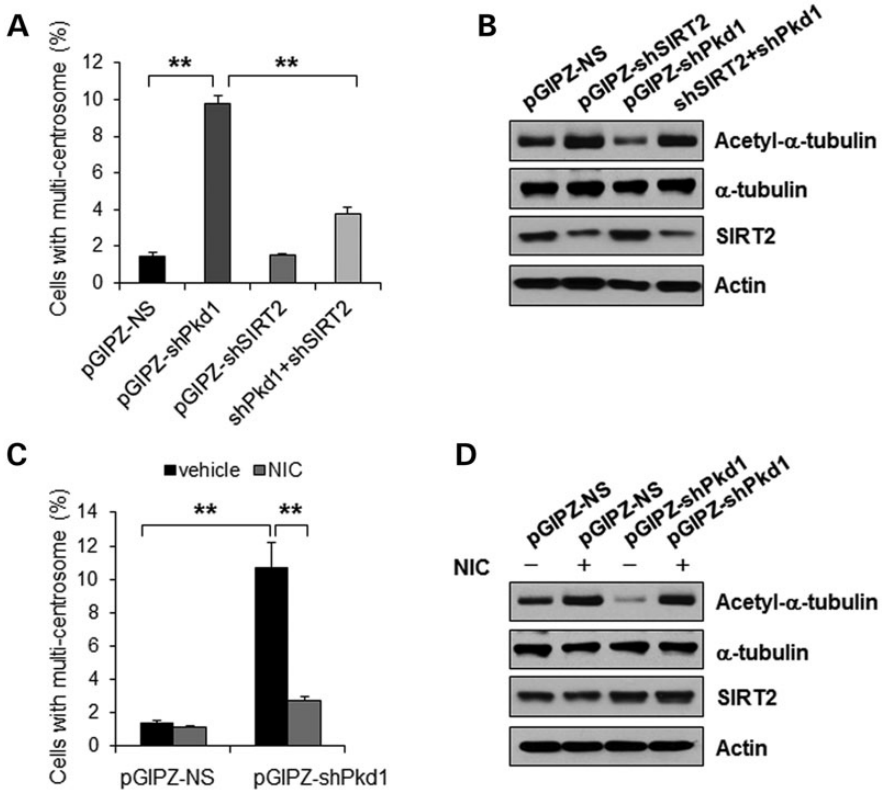

Figure 8. Aberrant centrosome amplification induced by loss of PC1 is mediated by SIRT2. (**A**) Mouse IMCD3 cells were transduced by Lentivector pGIPZ-NS, pGIPZ-shPkd1, pGIPZ-shSIRT2 or pGIPZ-shPkd1 plus pGIPZ-shSIRT2, respectively. The cells were stained with anti-γ-tubulin antibody, the centrosome marker. The percentage of cells with more than two centrosomes was counted. Error bars show the SD. ** $p < 0.01$. (**B**) Western blot analysis of the expression of acetylated α-tubulin, α-tubulin and SIRT2 in mouse IMCD3 cells transduced by Lentivector pGIPZ-NS, pGIPZ-shPkd1, pGIPZ-shSIRT2 or pGIPZ-shPkd1 plus pGIPZ-shSIRT2. Actin was used as a loading control. (**C**) Mouse IMCD3 cell transduced by Lentivector pGIPZ-NS or pGIPZ-shPkd1 were treated with 10 mM NIC for 48 h. The cells were stained with anti-γ-tubulin antibody, the centrosome marker. The percentage of cells with more than two centrosomes was counted. Error bars show the SD. **$P < 0.01$. (**D**) Western blot analysis of the expression of acetylated α-tubulin, α-tubulin and SIRT2 in NIC-treated mouse IMCD3 cells transduced by Lentivector pGIPZ-NS or pGIPZ-shPkd1, Actin was used as a loading control.

primary cilia in polycystic kidney disease (6,20) suggest that primary cilia and centrosomes are important in the process of cyst formation in PKD.

MATERIALS AND METHODS

Cell culture and reagents

Mouse IMCD3 cells and HEK293T cells were maintained at 37°C in 5% CO_2 in DMEM (Invitrogen, Carlsbad, CA, USA) supplemented with 10% fetal bovine serum (FBS). Dolichos biflorus agglutinin positive *Pkd1* wild-type and *Pkd1*$^{null/null}$ MEK cells were maintained as previously described (38). NIC was purchased from Sigma.

For analysis of ciliary assembly, cells were plated at 70% confluency in plates containing glass coverslips, and starved for 48 h (regular DMEM or DMEM F12 without serum) to induce cilia formation, followed by immunostaining. For analysis of ciliary disassembly, cells were plated at 30% confluency and starved for 48 h, followed by serum re-feeding.

Plasmids and mutagenesis

Mouse full-length SIRT2 was cloned into the pAcGFP-C1 vector (Clontech). Site-directed mutagenesis for SIRT2 constructs was performed with the QuickChange Kit Site-Directed Mutagenesis Kit (Stratagene, La Jolla, CA, USA) as recommended.

Western blotting and immunofluorescence

Western blotting was performed on whole-cell lysates as described by the manufacturer (Upstate Biotechnology, Lake Placid, NY, USA). The antibodies used for western blotting included anti-SIRT2 (Cell Signaling Technologies, Danvers, MA, USA 1:1000 dilution); anti-acetyl-α-tubulin, anti-α-tubulin and anti-actin antibodies (Sigma, St Louis, MO, USA, 1:5000 dilution). Donkey-anti-rabbit IgG-horseradish peroxidase and Donkey-anti-mouse IgG-horseradish peroxidase (Santa Cruz Biotechnology, Santa Cruz, CA, USA, 1:8000 dilution) were used as secondary antibodies for western blotting.

For immunofluorescence, confluent cells were grown on glass coverslips, rinsed with 1× phosphate-buffered saline (PBS), fixed with 4% paraformaldehyde containing 2% sucrose or methanol for 10 min and permeabilized with 1% Triton X-100 in PBS for 5 min. Anti-acetyl-α-tubulin (Sigma, St Louis, MO, USA, 1:10000 dilution), anti-pericentrin (Covance, Princeton, NJ, USA, 1:500 dilution), anti-SIRT2 (Sigma, St Louis, MO, USA, 1:500 dilution), anti-ARL13B (Proteintech, Chicago, IL,

USA, 1:1000 dilution), anti-BrdU (Sigma, St Louis, MO, USA, 1:1000 dilution) and anti-γ-tubulin (Sigma, St Louis, MO, USA, 1:500 dilution) were used for cell staining, respectively. The rabbit anti-pericentrin antibody (Covance, Princeton, NJ, USA, 1:1000 dilution) was also used for staining of the kidney tissues which were fixed with 4% paraformaldehyde (pH 7.4) from *Pkd1*$^{flox/flox}$*:Ksp-Cre* (39) mice, which was generated as previously described (40), and human ADPKD. Fluro 488-conjugated anti-mouse IgG antibody and Fluro 555 anti-rabbit IgG antibody (Invitrogen, Carlsbad, CA, USA) were used at a dilution of 1:10 000. Prolong anti-fade reagent (Invitrogen, Carlsbad, CA, USA) was used with DAPI. Immunofluorescence images were obtained with a NIKON ECLIPSE 80i Microscope.

RNA interference

The RNA oligonucleotides that specifically targeted mouse SIRT2 were purchased from Thermo Dharmacon. The RNA oligonucleotides were transfected with the DharmaFECT siRNA transfection reagent (Dharmacon). Forty-eight hours after transfection, cells were harvested and analyzed by western blotting.

Pkd1 and SIRT2 knockdown by lentivirus carrying *Pkd1* and SIRT2 shRNA

HEK293T cells were cotransfected with lentiviral plasmid pGIPZ-shPKD1 (Open Biosystems, Huntsville, AL, USA) carrying *Pkd1* shRNA, pGIPZ-shSIRT2 carrying SIRT2 shRNA or control empty vector pGIPZ-NS, psPAX2 packaging plasmid, and pMD2.G envelope plasmid, using calcium phosphate. Twelve hours later, medium containing the transfection reagent was removed and replaced with fresh complete DMEM medium plus 10% FBS and penicillin/streptomycin. Forty-eight hours later, cultures containing lentiviral particles were harvested from HEK293T cells. IMCD3 cells were then infected with appropriate amounts of lentiviral particles together with 5 μg/ml polybrene (Sigma, St Louis, MO). Twenty-four hours later, virus-containing medium was removed and replaced with fresh medium plus 10 μg/ml puromycin. Two days after selection, all the cells were GFP positive, which indicated the very high efficiency of transduction. Five days after infection, IMCD3 cells were harvested and analyzed by RT–PCR to examine the efficiency of *Pkd1* knockdown.

Quantitative reverse-transcription polymerase chain reaction

Total RNA was extracted using the RNeasy Plus Mini Kit (Qiagen, Germantown, MD, USA). One microgram of total RNA was used for reverse transcription reactions in a 20 μl reaction volume to synthesize cDNA using the iScript cDNA Synthesis Kit (Bio-Rad, Hercules, CA, USA). RNA expression profiles were analyzed by real-time PCR using iTaq SYBER Green Supermix with ROX (Bio-Rad) in an iCycler iQ Real-Time PCR Detection System. Genes were amplified using the following primers. Pkd1-F: 5′-TCAATTGCTCCGGCCGCTG-3′; Pkd1-R, 5′-CCAGCGTCTGAAGTAGGTTGTGGG-3′; Actin-F: 5′-AAGAGCTATGAGCTGCCTGA-3′; Actin-R: 5′-TACGGATGTCAACGTCACAC-3′. The complete reactions were subjected to the following program of thermal cycling: 40 cycles of 10 s at 95°C and 20 s at 63°C; a melting curve was run after the PCR cycles, followed by a cooling step. Each sample was run in triplicate in every experiment, and each experiment was repeated three times. The expression level of *Pkd1* was normalized to the expression level of actin.

Zebrafish experiments

Full-length mouse wild-type SIRT2 or SIRT2 mutation H187Y cDNA was cloned into pcDNA 3.0+ for *in vitro* transcription using the mMessage mMachine T7 Kit (Invitrogen, Carlsbad, CA, USA). The SIRT2 morpholino targeting either intron 1 and exon 2 splice site (5′-ACCTCTAAAGGACACAAAAAAGGCT-3′, 7.5 ng) or exon 3 and intron 3 splice site (5′-GTACGTGTTTGTCACATACTCTCA-3′, 7.5 ng) or standard control morpholino (5′-CCTCTTACCTCAGTTACAATTTATA-3′, 7.5 ng) provided by Gene Tools, or mRNA (50 pg) was injected into one-cell stage embryos using a Nanoliter 2000 microinjector (World Precision Instruments, Sarasota, FL, USA). The primers flanking exon 1 and exon 4 (forward: 5′-GCTGGCTTATAGTTTTAAAGAGGGTA-3′; reverse: 5′-AGTATGTAGCGAGCAACTGAGTC-3′) and the primers flanking exon 1 and exon 5 (forward: 5′-GCTGGCTTATAGTTTTAAAGAGGGTA-3′; reverse: 5′-GCTCCAACCATACAGATAATGTTC-3′) were employed in the subsequent RT–PCR to verify the splice blockage of the morpholino. For whole mount immunofluorescence, the embryos at 10-SS were fixed with 4% formaldehyde in PBS at 4°C overnight and transferred to 100% methanol for 2 h at −20°C followed by an overnight at 4°C. After rehydrating the embryos, they were washed in PBS with 0.1% Tween-20 and blocked in PBS-DBT (1 × PBS, 1% BSA, 10% normal goat serum and 0.1% Tween-20) at room temperature for 2 h, followed by antibody staining for acetylated α-tubulin (1:1000) at 4°Covernight. After 4× per 30 min washes in PBTw (1 × PBS/0.1 Tween-20), the embryos were incubated with Alexa Fluor 488-labeled goat anti-mouse IgG antibody (Invitrogen, Carlsbad, CA, USA, 1:10000 dilution) for 2 h at room temperature. After washing, the tail region of the embryos was removed and mounted. Embryos were imaged using a NIKON ECLIPSE 80i Microscope with a ×60 objective.

Data analysis

All quantifiable data are reported as means ± SEM. Comparison between two groups was carried out using an unpaired two-tailed Student's t test. The difference between two groups was statistically significant at P-values <0.05.

SUPPLEMENTARY MATERIAL

Supplementary Material is available at *HMG* online.

Conflict of Interest statement: none interest.

FUNDING

X.L. acknowledges support from the PKD Foundation, Children's Research Institute, and National Institutes of Health

(NIH) grant R01DK084097. R.R. acknowledges support from NIH grant HL090712. J.P.C. acknowledges support from NIH grant P50DK057301. K.L. acknowledges partial support by an AHA post-doctoral fellowship award.

REFERENCES

1. Cano, D.A., Murcia, N.S., Pazour, G.J. and Hebrok, M. (2004) Orpk mouse model of polycystic kidney disease reveals essential role of primary cilia in pancreatic tissue organization. *Development*, **131**, 3457–3467.
2. Huangfu, D. and Anderson, K.V. (2005) Cilia and Hedgehog responsiveness in the mouse. *Proc. Natl Acad. Sci. USA*, **102**, 11325–11330.
3. Tanaka, Y., Okada, Y. and Hirokawa, N. (2005) FGF-induced vesicular release of sonic hedgehog and retinoic acid in leftward nodal flow is critical for left-right determination. *Nature*, **435**, 172–177.
4. Davenport, J.R., Watts, A.J., Roper, V.C., Croyle, M.J., van Groen, T., Wyss, J.M., Nagy, T.R., Kesterson, R.A. and Yoder, B.K. (2007) Disruption of intraflagellar transport in adult mice leads to obesity and slow-onset cystic kidney disease. *Curr. Biol.*, **17**, 1586–1594.
5. Holland, A.J. and Cleveland, D.W. (2009) Boveri revisited: chromosomal instability, aneuploidy and tumorigenesis. *Nat. Rev. Mol. Cell Biol.*, **10**, 478–487.
6. Battini, L., Macip, S., Fedorova, E., Dikman, S., Somlo, S., Montagna, C. and Gusella, G.L. (2008) Loss of polycystin-1 causes centrosome amplification and genomic instability. *Hum. Mol. Genet.*, **17**, 2819–2833.
7. Dutcher, S.K. (2001) The tubulin fraternity: alpha to eta. *Curr. Opin. Cell. Biol.*, **13**, 49–54.
8. Bobinnec, Y., Khodjakov, A., Mir, L.M., Rieder, C.L., Edde, B. and Bornens, M. (1998) Centriole disassembly in vivo and its effect on centrosome structure and function in vertebrate cells. *J. Cell Biol.*, **143**, 1575–1589.
9. Garcia-Gonzalo, F.R. and Reiter, J.F. (2012) Scoring a backstage pass: mechanisms of ciliogenesis and ciliary access. *J. Cell Biol.*, **197**, 697–709.
10. Kobayashi, T. and Dynlacht, B.D. (2011) Regulating the transition from centriole to basal body. *J. Cell Biol.*, **193**, 435–444.
11. Pan, J. and Snell, W. (2007) The primary cilium: keeper of the key to cell division. *Cell*, **129**, 1255–1257.
12. Matsuyama, A., Shimazu, T., Sumida, Y., Saito, A., Yoshimatsu, Y., Seigneurin-Berny, D., Osada, H., Komatsu, Y., Nishino, N., Khochbin, S. *et al.* (2002) In vivo destabilization of dynamic microtubules by HDAC6-mediated deacetylation. *EMBO J*, **21**, 6820–6831.
13. Shida, T., Cueva, J.G., Xu, Z., Goodman, M.B. and Nachury, M.V. (2010) The major alpha-tubulin K40 acetyltransferase alphaTAT1 promotes rapid ciliogenesis and efficient mechanosensation. *Proc. Natl Acad. Sci. USA*, **107**, 21517–21522.
14. Pugacheva, E.N., Jablonski, S.A., Hartman, T.R., Henske, E.P. and Golemis, E.A. (2007) HEF1-dependent Aurora A activation induces disassembly of the primary cilium. *Cell*, **129**, 1351–1363.
15. North, B.J. and Verdin, E. (2007) Interphase nucleo-cytoplasmic shuttling and localization of SIRT2 during mitosis. *PloS ONE*, **2**, e784.
16. North, B.J., Marshall, B.L., Borra, M.T., Denu, J.M. and Verdin, E. (2003) The human Sir2 ortholog, SIRT2, is an NAD^+-dependent tubulin deacetylase. *Mol. Cell*, **11**, 437–444.
17. Nahhas, F., Dryden, S.C., Abrams, J. and Tainsky, M.A. (2007) Mutations in SIRT2 deacetylase which regulate enzymatic activity but not its interaction with HDAC6 and tubulin. *Mol. Cell Biochem.*, **303**, 221–230.
18. Caspary, T., Larkins, C.E. and Anderson, K.V. (2007) The graded response to sonic Hedgehog depends on cilia architecture. *Dev. Cell*, **12**, 767–778.
19. Essner, J.J., Amack, J.D., Nyholm, M.K., Harris, E.B. and Yost, H.J. (2005) Kupffer's vesicle is a ciliated organ of asymmetry in the zebrafish embryo that initiates left-right development of the brain, heart and gut. *Development*, **132**, 1247–1260.
20. AbouAlaiwi, W.A., Ratnam, S., Booth, R.L., Shah, J.V. and Nauli, S.M. (2010) Endothelial cells from humans and mice with polycystic kidney disease are characterized by polyploidy and chromosome segregation defects through survivin down-regulation. *Hum. Mol. Genet.*, **20**, 354–367.
21. Plotnikova, O.V., Pugacheva, E.N. and Golemis, E.A. (2009) Primary cilia and the cell cycle. *Methods Cell Biol.*, **94**, 137–160.
22. Zhang, Y., Kwon, S., Yamaguchi, T., Cubizolles, F., Rousseaux, S., Kneissel, M., Cao, C., Li, N., Cheng, H.L., Chua, K. *et al.* (2008) Mice lacking histone deacetylase 6 have hyperacetylated tubulin but are viable and develop normally. *Mol. Cell. Biol.*, **28**, 1688–1701.
23. Kim, H.S., Vassilopoulos, A., Wang, R.H., Lahusen, T., Xiao, Z., Xu, X., Li, C., Veenstra, T.D., Li, B., Yu, H. *et al.* (2011) SIRT2 Maintains genome integrity and suppresses tumorigenesis through regulating APC/C activity. *Cancer Cell*, **20**, 487–499.
24. Dryden, S.C., Nahhas, F.A., Nowak, J.E., Goustin, A.S. and Tainsky, M.A. (2003) Role for human SIRT2 NAD-dependent deacetylase activity in control of mitotic exit in the cell cycle. *Mol. Cell. Biol.*, **23**, 3173–3185.
25. North, B.J. and Verdin, E. (2007) Mitotic regulation of SIRT2 by cyclin-dependent kinase 1-dependent phosphorylation. *J. Biol. Chem.*, **282**, 19546–19555.
26. Clement, A., Solnica-Krezel, L. and Gould, K.L. (2011) The Cdc14B phosphatase contributes to ciliogenesis in zebrafish. *Development*, **138**, 291–302.
27. Quarmby, L.M. and Parker, J.D. (2005) Cilia and the cell cycle? *J. Cell Biol.*, **169**, 707–710.
28. Kim, S., Zaghloul, N.A., Bubenshchikova, E., Oh, E.C., Rankin, S., Katsanis, N., Obara, T. and Tsiokas, L. (2011) Nde1-mediated inhibition of ciliogenesis affects cell cycle re-entry. *Nat. Cell Biol.*, **13**, 351–360.
29. Chuang, J.Z., Yeh, T.Y., Bollati, F., Conde, C., Canavosio, F., Caceres, A. and Sung, C.H. (2005) The dynein light chain Tctex-1 has a dynein-independent role in actin remodeling during neurite outgrowth. *Dev. Cell*, **9**, 75–86.
30. Li, A., Saito, M., Chuang, J.Z., Tseng, Y.Y., Dedesma, C., Tomizawa, K., Kaitsuka, T. and Sung, C.H. (2011) Ciliary transition zone activation of phosphorylated Tctex-1 controls ciliary resorption, S-phase entry and fate of neural progenitors. *Nat. Cell Biol.*, **13**, 402–411.
31. Robert, A., Margall-Ducos, G., Guidotti, J.E., Bregerie, O., Celati, C., Brechot, C. and Desdouets, C. (2007) The intraflagellar transport component IFT88/polaris is a centrosomal protein regulating G1-S transition in non-ciliated cells. *J. Cell Sci.*, **120**, 628–637.
32. Qin, H., Wang, Z., Diener, D. and Rosenbaum, J. (2007) Intraflagellar transport protein 27 is a small G protein involved in cell-cycle control. *Curr. Biol.*, **17**, 193–202.
33. Jackson, P.K. (2011) Do cilia put brakes on the cell cycle?. *Nat. Cell Biol.*, **13**, 340–342.
34. Winyard, P. and Jenkins, D. (2011) Putative roles of cilia in polycystic kidney disease. *Biochim. Biophys. Acta*, **1812**, 1256–1262.
35. Hopp, K., Ward, C.J., Hommerding, C.J., Nasr, S.H., Tuan, H.F., Gainullin, V.G., Rossetti, S., Torres, V.E. and Harris, P.C. (2012) Functional polycystin-1 dosage governs autosomal dominant polycystic kidney disease severity. *J. Clin. Invest.*, **122**, 4257–4273.
36. Cowley, D.O., Rivera-Perez, J.A., Schliekelman, M., He, Y.J., Oliver, T.G., Lu, L., O'Quinn, R., Salmon, E.D., Magnuson, T. and Van Dyke, T. (2009) Aurora-A kinase is essential for bipolar spindle formation and early development. *Mol. Cell. Biol.*, **29**, 1059–1071.
37. Wang, X., Zhou, Y.X., Qiao, W., Tominaga, Y., Ouchi, M., Ouchi, T. and Deng, C.X. (2006) Overexpression of aurora kinase A in mouse mammary epithelium induces genetic instability preceding mammary tumor formation. *Oncogene*, **25**, 7148–7158.
38. Li, X., Luo, Y., Starremans, P.G., McNamara, C.A., Pei, Y. and Zhou, J. (2005) Polycystin-1 and polycystin-2 regulate the cell cycle through the helix-loop-helix inhibitor Id2. *Nat. Cell Biol.*, **7**, 1202–1212.
39. Shao, X., Somlo, S. and Igarashi, P. (2002) Epithelial-specific Cre/lox recombination in the developing kidney and genitourinary tract. *J. Am. Soc. Nephrol.*, **13**, 1837–1846.
40. Zhou, X., Fan, L.X., Sweeney, W.E. Jr., Denu, J.M., Avner, E.D. and Li, X. (2013) Sirtuin 1 inhibition delays cyst formation in autosomal-dominant polycystic kidney disease. *J. Clin. Invest.*, **123**, 3084–3098.